

Electron orbital energies of oxygen adsorbed on silicon surfaces and of silicon dioxide

H. Ibach* and J. E. Rowe

Bell Laboratories, Murray Hill, New Jersey 07974

(Received 24 January 1974)

The electronic structures of oxygen adsorbed on silicon (111) 2×1 cleaved, (111) 7×7 , and (100) 2×1 surfaces and of oxidized silicon have been investigated by combining electron energy-loss spectroscopy (ELS) and ultraviolet photoemission spectroscopy (UPS). In addition the surfaces were characterized by Auger electron spectroscopy (AES) and low-energy electron diffraction (LEED). The electronic spectra are discussed in terms of localized *s*- and *p*-like bonds. For adsorbed oxygen one *s*-like and four *p*-like electron states are found. The structure of the surface layer is amorphous. The energies of the electron states (UPS) as well as the transition energies (ELS) were found to be almost independent of face and surface structure. Silicon can be oxidized to form a SiO₂-type oxygen bond by either annealing or electron bombarding the oxygen-covered surface or by bombardment with oxygen ions. For SiO₂, three *2p* levels and one *2s* level are found as expected. The electron states are compared to those of the H₂O molecule. Important final states for transitions observed in ELS seem to be excitons near the bottom of the silicon conduction-band minimum for adsorbed oxygen and ~ 1.5 eV below the conduction band for SiO₂.

I. INTRODUCTION

An understanding of chemisorption on solid surfaces is at the present time in a very early stage of development. Basic structural parameters such as bond lengths and angles of chemisorbed atoms and molecules are not known in general. Thus, it is useful to correlate experimental data from several different methods used *in situ* on the same sample in order to attempt to understand a particular chemisorption process. In this paper we describe experiments on the chemisorption of oxygen on silicon (111) and (100) surfaces. The electronic states of adsorbed oxygen are studied from submonolayer concentrations to multilayer concentrations involving the formation of bulk silicon dioxide. The well established techniques of low-energy electron diffraction (LEED) and Auger electron spectroscopy (AES) were used to control the preparation of surfaces and adsorbate layers. The electron states were then investigated by ultraviolet photoemission spectroscopy (UPS) and electron energy-loss spectroscopy (ELS). It seems generally accepted that for far-ultraviolet photon energies ($\hbar\omega \sim 20$ eV), peaks in the photoemission density of states correspond to peaks in the true density of occupied states, though matrix-element and angular effects may influence the relative intensities.

The interpretation of ELS is somewhat less straightforward. Due to the dependence on both real and imaginary parts of the optical dielectric function, $\epsilon(\omega)$, the one-electron-like peaks in ELS may be shifted compared to the actual interband transition energies. This is especially true if the transition energies are close to the energy of a collective excitation. It has been shown,¹ however, that for sharp adsorbate-associated transitions the shift is small for low coverages. A combination of

UPS and ELS then reveals information about the unoccupied final states. Furthermore, ELS can probe deep-lying states of adsorbates not accessible to UPS.

The adsorption of oxygen on silicon has been of considerable interest for many years. Despite the technical importance of the oxidation process, details of the adsorption were not understood and contradictory results have been obtained. By combining the methods of Auger electron spectroscopy, ellipsometry, and electron spectroscopy of surface vibrations we have shown recently that these difficulties were caused by the presence of surface-step irregularities, which control the adsorption kinetics.^{2,3} It has been shown further that adsorbed oxygen up to a coverage of a monolayer is in a binding state different from that in SiO₂. Although the available data could not give a clear answer to the question of the structure of adsorbed oxygen, several models based on dissociative adsorption could be excluded and a peroxide-bridge model has been proposed. The differences in chemical bonding and geometrical structure for oxygen in the two binding states (adsorbed oxide and SiO₂) should show up in different energies of the bonding electrons. In fact, distinctive differences in the energy-loss spectra have been observed for the two cases.¹ On the other hand, no differences were found in the loss spectra for different crystal faces [(111), (100), and (110)] covered with oxygen, and the adsorbed oxygen has a disordered LEED pattern. Therefore, one bond model should apply to the adsorption of oxygen on all low-index surfaces. Without the results of UPS, however, an understanding of the nature of the observed transitions could not be achieved. In this paper UPS spectra as well as an extension of the ELS data to higher

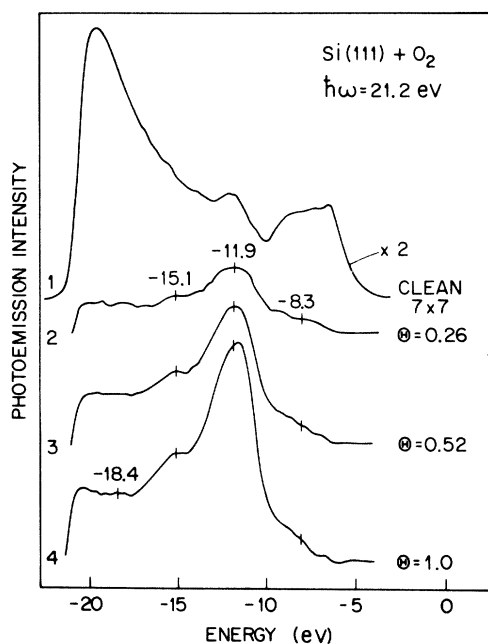


FIG. 1. Photoemission spectra of silicon (111) surfaces at $\hbar\omega = 21.2$ eV for 100 eV pass energy. Curve 1 is the spectrum of the clean 7×7 surface. Clean surface features are not as well resolved as in other data at 50 eV pass energy (Ref. 7). Curves 2-4 show the difference between the surface exposed to oxygen and the clean surface for increasing coverage. The positions of the oxygen peaks are independent of coverage.

loss energies will be presented. A comparison of the results will lead us to a detailed description of the electron orbital energies of adsorbed oxygen and of amorphous SiO_2 .

II. EXPERIMENTAL TECHNIQUES

The vacuum system consisted of an ion-pumped stainless-steel chamber, with the electron spectrometers and the LEED system mounted on three different ports. The base pressure was $\sim 5\times 10^{-11}$ Torr. A single-pass PHI 10-234G cylindrical-mirror analyzer was used for AES and ELS. The AES spectra were taken as the first derivative dN/dE of the energy distribution while for the ELS spectra the second derivative $-d^2N/dE^2$ has been found to be more useful.⁴ The light source for the photoemission was a differentially pumped microwave resonance lamp.⁵ The lamp was operated on the He I 21.2-eV and the He II 40.8-eV lines at a pressure of 1 and 0.3 Torr, respectively. The photoelectrons were analyzed with a PHI 15-250 double-pass analyzer operated in the retard mode corresponding to a constant resolution of ≤ 0.5 eV. A small bias could be applied to the sample to insure that even the slowest electrons were able to enter the analyzer. In this paper all energies in the UPS spectra will be referred to the vacuum

level $E_{\text{vac}} = 0$. The point $E = -\hbar\omega$ was determined by a linear extrapolation of the slow secondary peak to zero kinetic energy. The error introduced by this procedure is estimated to be smaller than ± 0.2 eV.

Clean silicon surfaces were prepared by argon bombardment and annealing or by cleaving in a multiple cleaving tool. Details of the manipulator and cleaving tool have been described elsewhere.⁶ Oxygen was admitted by a leak valve connected to a standard silver leak. The partial pressure of oxygen compared to the residual gas (especially CO and noble gases released from the pump) was monitored by an EAI model 1100 quadrupole mass spectrometer. The effects of any CO partial pressure were negligible due to additional pumping by a liquid-nitrogen-temperature titanium sublimation pump. Occasionally very small amounts of carbon contamination (< 0.05 monolayer) were detected after the oxygen adsorption to one monolayer or greater was completed. The oxygen adsorption is known to saturate at exposures between 10 and 10^3 L ($\mu\text{torr sec}$). The necessary exposure depends on the surface roughness (e.g., cleavage steps)² that control the sticking coefficient. The same amount of oxygen independent of surface roughness is adsorbed by all surfaces.² As a matter of convenience we call this amount "monolayer coverage" in the following sections in agreement with gas-volumetric measurements.

III. RESULTS

A. General experimental observations

As reported earlier,^{8,9} the LEED pattern of surfaces covered with a monolayer of oxygen is diffuse with weak integral-order diffracted beams appearing only at certain energies. This indicates an amorphous surface layer. No significant differences between the different surfaces were found in either the LEED pattern or the UPS and the ELS data.

B. Ultraviolet photoemission spectra

Figure 1 shows the photoemission spectrum of a clean silicon (111) 7×7 surface (curve 1). Data for adsorbed oxygen (see curves 2-4) are shown as difference spectra between the adsorbed and the clean surfaces for various coverages. The photoyield from the oxygen-associated states at $\theta \approx 1$ mono-layer is about five times the yield from the states of the clean surface. Four peaks at -8.3, -11.9, -15.1, and -18.4 eV are found for adsorbed oxygen (see Figs. 1 and 2). In contrast with the states for the adsorbed monolayer of oxygen, UPS results for silicon-dioxide films show only three peaks at -13.2, -17.1, and -20.4 eV. The transition between these two spectra was studied by controlled oxidation of silicon surfaces

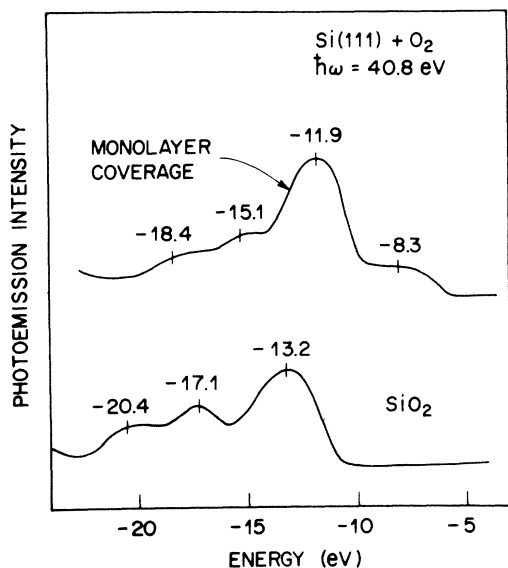


FIG. 2. Photoemission spectra of silicon surfaces covered with a monolayer of oxygen and silicon dioxide for $\hbar\omega = 40.8$ eV.

with an adsorbed monolayer.

Oxidation of silicon about $\theta = 1$ was achieved by heating the samples in an oxygen atmosphere, by electron bombardment and oxygen exposure,^{1,2} or

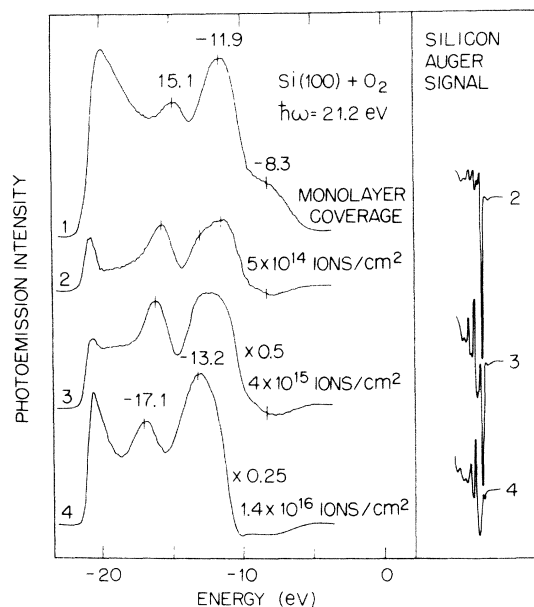


FIG. 3. Photoemission spectra for $\hbar\omega = 21.2$ eV. Curve 1 corresponds to a monolayer coverage with oxygen. Curves 2-4 show the difference between surfaces sputtered with an increasing dose of oxygen ions and the monolayer-covered surface. On curve 4 the peak positions of the fully oxidized surface (Fig. 2) are indicated. The silicon *L*VV Auger signal is shown for comparison.

by bombardment with 500-eV O_2^+ ions. No differences in ELS and UPS spectra were found between the three different methods of oxidation. In Figs. 3 and 4 we show the results for O_2^+ bombardment. Curve 1 shows a silicon surface with a coverage of a monolayer. Curves 2-4 are the differences due to increasing oxygen-ion bombardment. The total number of ions divided by the sample area are given for each curve. Assuming a sticking coefficient of one for oxygen ions an average of $\theta = 2.3$ is calculated for curve 2. This is in reasonable agreement with a coverage determination of $\theta = 1.8$ from the oxygen *KLL* Auger-signal peak height measured at the center of the sample. The coverages for curves 3 and 4 in Fig. 3 can therefore be estimated to $\theta = 7.5$ and $\theta = 23$ corresponding to a thickness of the SiO_2 layers of 11 and 34 Å, respectively. The silicon *L*VV Auger signal in arbitrary units are given in Fig. 3 for comparison. While the silicon AES signal for a surface covered with a monolayer of oxygen has still almost the same shape as the silicon signal of a clean surface, the silicon signal of SiO_2 is quite different due to the changes in the valence-band structure. This difference has been already observed earlier.¹⁰ The differences in the electron

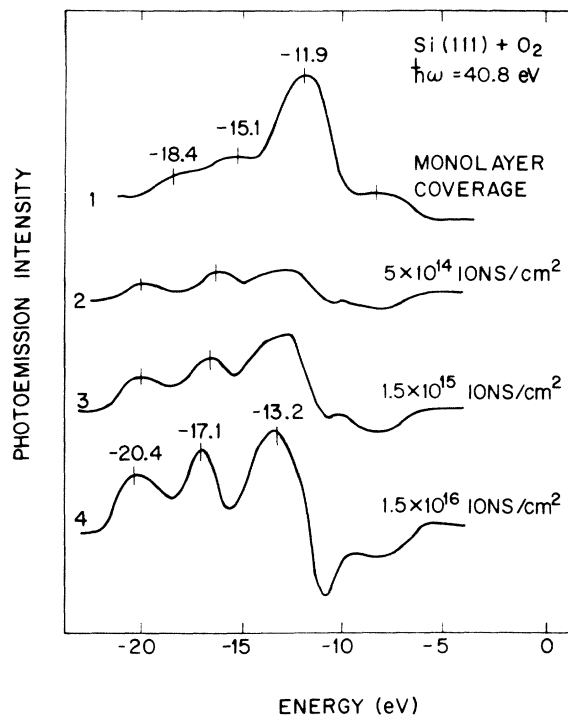


FIG. 4. Photoemission spectra for $\hbar\omega = 40.8$ eV. Curves 2-4 show the difference between surfaces sputtered with an increasing dose of oxygen ions. The negative part of curve 4 indicates that the states of the adsorbed oxygen are removed during oxidation.

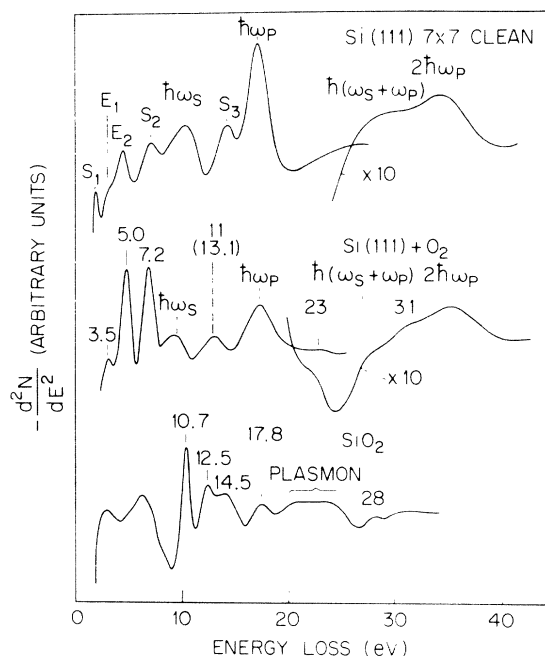


FIG. 5. Negative second derivative of the energy-loss spectra of a clean silicon (111) 7×7 surface, the same surface covered with adsorbed oxygen $\Theta \approx 0.7$, and silicon dioxide. The energy of the electron beam was 100 eV. For the oxygen-associated losses the transition energies are given in the figure. Only for the 13.1-eV loss is a considerable dielectric shift observed.¹ The energy losses can be attributed to transitions from oxygen p and s levels (see also Tables I and II).

energy levels of the $\text{Si} + \text{O}_2$ and the SiO_2 system are clearly seen in the UPS spectra. Increasing oxidation removes the -8.3 -eV peak and apparently somewhat later the -11.9 -eV peak and adds new peaks at -13.2 , -17.1 , and -20.4 eV. There seems to be a slight shift in the positions of the SiO_2 peaks with increasing oxidation. The ratio of the photoyields of the oxidized silicon relative to the monolayer-covered surface for the 40.8-eV radiation is \sim three times smaller than for 21.2 eV (see scale factors in Figs. 3 and 4). This is probably due to the smaller photoelectron-escape depth and different optical matrix-element effects at 40.8 eV.

C. Electron energy loss spectra

Second-derivative energy-loss spectra of the clean (111) 7×7 , the oxygen covered, and the oxidized silicon surface are shown in Fig. 5. A detailed description of the spectra of the clean surfaces has been given elsewhere¹¹ and shall only be briefly summarized here. The transitions marked by $\hbar\omega_s$ and $\hbar\omega_p$ are surface- and bulk-plasmon excitations, respectively. The energy of the surface plasmon is slightly different for different surface oxidations. So are the energies of the "bulk" inter-

band transitions E_1 and E_2 . S_1 , S_2 , and S_3 are transitions from surface states. The initial state for S_1 is the dangling-bond surface state¹¹ at the top of the valence band that is also found in photoemission,^{7,12,13} The occupied states for S_2 and S_3 are surface states at the bottom of the p -like and s -like valence bands, respectively, and are associated with a strengthening of the backbonds of the silicon surface atoms.¹⁴ In the high-energy regime two double-plasma losses are seen. Their expected positions are marked at $\Delta E = \hbar(\omega_s + \omega_p) = 27.9$ eV and $\Delta E = 2\hbar\omega_p = 34.8$ eV. On the oxygen-covered surface ($\Theta \approx 0.7$) the surface plasmon is shifted from 10.5 to 9.7 eV.¹ Therefore, the double loss $\hbar(\omega_s + \omega_p)$ appears at a smaller energy of 27.1 eV. The energy losses due to adsorbed oxygen are marked by their transition energies. The 3.5-eV and the 5.0-eV peaks occur at approximately the same energy as the E_1 and E_2 transitions on the clean surfaces. Loss spectroscopy alone presents therefore, no clear evidence that these peaks are due to transitions from oxygen-derived electronic states. One could as well interpret these as silicon interband transitions which appear sharper on oxygen-covered surfaces. Like other transitions the 7.2-eV peak appears in the same relative height on the (100) 2×1 surface (see Fig. 6) where the S_2

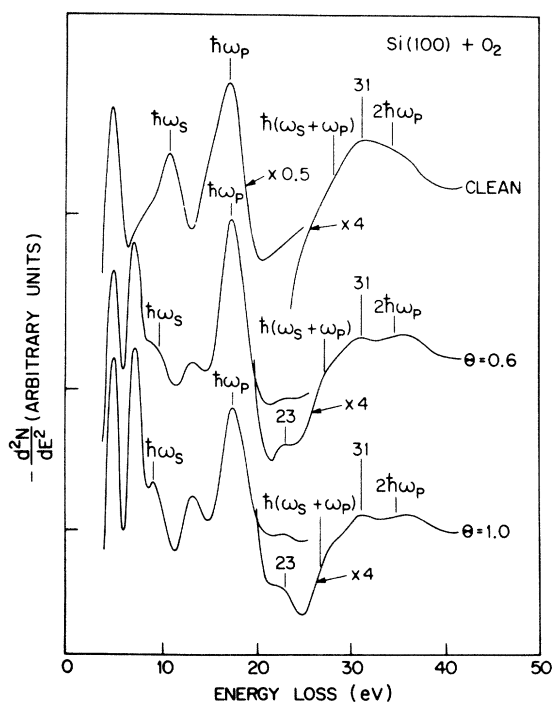


FIG. 6. Negative second derivative of the energy-loss spectra of a clean silicon (100) 2×1 surface and the same surface covered with oxygen. The energy of the electron beam was 80 eV. The 31-eV transition appears also on the clean surface.

transition is only very weak. It has therefore been concluded that the initial state for this transition is an oxygen electronic level.¹ A considerable dielectric shift from ~ 11 eV at low coverages to ~ 13.2 eV for a monolayer coverage is observed for the 11-eV transition.¹ At higher loss energies two additional peaks at 23 and 31 eV are observed after oxygen adsorption. The 23-eV peak has never been observed on the clean surfaces independent of the incident electron energy. At 80-eV incident electron energy, however, a broad structure is observed around 31-eV loss energy (see Fig. 6) on both the (111) and (100) surfaces. At the same energy the double plasma losses do not seem to appear at their expected positions. Increasing oxygen coverage sharpens the peak at 31 eV. The intensity of the loss peak at 23 eV is proportional to the oxygen coverage as are the peaks at 7.2 and 11 eV.

The loss spectrum for a completely oxidized surface (SiO_2) is shown in Fig. 5. It has been shown that the observed second-derivative loss spectrum agrees quite well with the second derivatives of the bulk- and surface-loss function, $-d^2\text{Im}(1/\epsilon)/dE^2$ and $-d^2\text{Im}[1/(\epsilon+1)]/dE^2$.¹ The dielectric function, $\epsilon(\omega)$, of SiO_2 is very different from the quasifree electron-like, $\epsilon(\omega)$, of silicon. The real part of $\epsilon(\omega)$ is positive in the entire range above 8 eV.¹⁵ Bulk- and surface-loss functions are therefore quite similar and instead of well defined surface- and bulk-plasma losses only a broad double structure centered near 22 eV is observed. The single-particle electronic transitions for SiO_2 are indicated by their energies, 10.7, 12.5, 14.5, 17.8, and 28 eV.

IV. DISCUSSION

Photoemission spectra and energy-loss spectra demonstrate that the electron states of adsorbed oxygen and SiO_2 are very different. This is in agreement with earlier observations.^{2,3,10} In the following we shall discuss the electron states of the adsorbed oxygen and the results for SiO_2 shall be discussed in Sec. IV B.

A. Electronic structure of the adsorbed oxygen monolayer

The photoemission spectra of adsorbed oxygen (Figs. 1–4) exhibit four peaks at -18.4 , -15.1 , -11.9 , and -8.3 eV. No shifts in the peak positions with increasing coverage in the submonolayer range $\Theta \leq 1$ are observed (see Fig. 1). Also the relative intensities of the different peaks do not change with exposure. It is therefore concluded that oxygen adsorbs in a single-binding state. This is in agreement with the observations of the vibrational spectrum.² The silicon-oxygen bond is strongly localized and therefore the structure in

the density of states should reflect the localized molecular orbitals of the surface-adsorbate complex. Thus, peak positions in the photoemission spectrum are expected to represent to a good approximation these molecular-orbital energies. If the UPS peaks were caused by matrix-element effects, more dramatic changes in the spectra would occur when the photon energy is varied between 21.2 and 40.8 eV. For atomic oxygen the energies of the 2s and 2p orbitals are well separated with energies of -30 and -13.6 eV, respectively.¹⁶ Therefore, the four peaks in the photoemission spectra discussed above represent (at least) four different 2p-like orbitals of adsorbed oxygen. The adsorption is either nondissociative or after dissociation the two oxygen atoms are bound in different sites at the surface. The latter possibility is considered very unlikely since the different energies of the two sites would imply a sequential filling during adsorption, whereas we observe only a single-adsorption step consistent with a single-adsorption site.

The energy-loss spectra of oxygen-covered silicon surfaces exhibit peaks at 3.5, 5, 7.2, 13.1, 23, and 31 eV in addition to the bulk- and surface-plasmon peaks. The peaks at 7.2, 13 (11 at small coverages)¹ and 23 eV have been observed for primary energies between 50–200 eV. Their intensities increase with increasing coverage and no comparable transitions are observed on the clean surfaces at any primary energy. These energy losses are attributed to transitions from occupied to unoccupied electron states in the oxygen-silicon surface layer. The peaks at 3.5 and 5.0 eV on the oxygen-covered surface occur at approximately the energy as the E_1 and E_2 transitions of the clean surface. One might consider the 3.5 and the 5 eV loss of the oxygen-covered surface to be sharpened interband transitions of silicon. This interpretation, however, is not particularly likely, since the change from the crystalline to the amorphous silicon surface would rather tend to weaken the structure of bulk interband transitions. This is in fact observed for surfaces disordered by argon bombardment.¹¹ We therefore assume that the 3.5- and 5-eV transition are oxygen-associated transitions as well. The peak at 31 eV is probably not due to an oxygen transition, since depending on the primary energy the same peak (Fig. 6) is sometimes observed even on the clean surfaces [(111) and (100)]. The nature of this peak is not yet understood.

Having established the energies of the surface orbitals and the transition energies one may try to combine this information and can possibly arrive at some conclusions about the final states that are involved in the observed electronic transitions. Such an attempt is made in Fig. 7 for three of the ob-

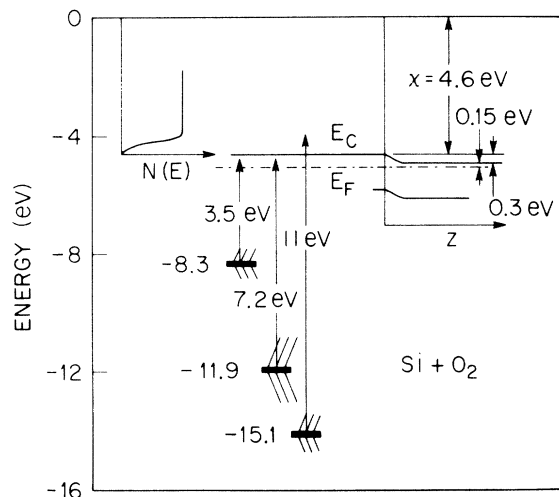


FIG. 7. Comparison of peaks in the photoemission density of oxygen states and the transition energies obtained from loss spectroscopy. The inserts show the band bending at the surface and the conduction-band density of states for amorphous silicon.

served transitions. The inserts in Fig. 7 display the density of states of amorphous silicon¹⁷ and the surface-band bending. The electron affinity was determined by a linear extrapolation of the valence-band photoemission density of states for the oxygen-covered surface. The conduction-band density of states is structureless (apart from the step at the bottom) due to the lack of long-range order.¹⁷ The energy-loss spectrum (Fig. 5) shows the oxygen transitions as peaks rather than steplike shapes. Therefore, the final state must have a well defined energy. We believe that this final state is an excitation at the bottom of the conduction band. This assumption is confirmed by observations of Brown and Rustgi,¹⁸ who measured the absorption coefficient of amorphous bulk silicon near $\hbar\omega = 100$ eV. The absorption due to excitations from the L_{II} - and L_{III} -core levels into the conduction band exhibits an excitonic enhancement for transitions to the bottom of the conduction band. Exciton lines are not resolved because of the dielectric screening in the solid.¹⁸ Screening, however, is expected to be smaller at the surface and a sharper peak may result.

The origin of the 5.0-eV transition is not yet understood, but it may be due to transitions from the broad UPS band (-8.3 to -10.5 eV) to the same excitonic final state as the 3.5, 7.2, and 11-eV transitions. It is surprising that no transition is observed from the -18.4 -eV state. This might be a result of the much larger width (approximately a factor of two) compared to the -15.1 -eV state (see Fig. 2) which would reduce the second-derivative signal by a factor of four. A deeper

initial state is usually lifetime broadened considerably since the lifetime broadening increases rapidly with increasing transition energy.

It seems clear from Figs. 5 and 6 that the 23-eV loss peak corresponds to an oxygen electronic transition as well, while this is doubtful for the 31-eV peak. Assuming the final state for the 23-eV transition to be the same as that for the three transitions in Fig. 7 the energy of the initial state can be calculated (Table I). The 3s and 3p states of silicon form a 12-eV-wide band between -5 and -17 eV. It seems likely therefore that the low orbital at -28 eV is a 2s-like oxygen orbital.

It should be mentioned that little arbitrariness is involved in the assignment proposed above, since the final state is expected to lie somewhere between the Fermi level and the vacuum level. Right at the surface no final states of sufficiently long lifetime should exist at energies above the vacuum level because of the strong coupling to propagating waves.¹⁹

B. Electronic structure of silicon dioxide

The photoemission-difference spectra at the beginning of the oxidation (see curves 2 and 3 of Fig. 3) are rather complicated. While the intensity of the -8.3 -eV peak of adsorbed oxygen is gradually decreased with further oxidation the -11.9 -eV peak seems to be still increasing. The -11.9 -eV peak is also removed eventually as indicated by the negative peak in the difference curve at 11 eV shown in Fig. 4. This different behavior might be caused by changes in matrix elements due to the changes in the surface electronic structure with increasing oxidation. The final result, however, is quite clear. Essentially no oxygen in the adsorbed monolayer state is present on amorphous SiO_2 , since the intensity at -8.3 eV is almost completely removed. Further, a comparison of the second derivative of $-1m1/\epsilon$ calculated from the bulk dielectric function, $\epsilon(\omega)$, agrees with the second-derivative loss spectrum.¹ The energies of the SiO_2 surface orbitals are therefore very close to their bulk values. As in the case of adsorbed oxygen, the initial states for the observed transi-

TABLE I. Energies of surface bond orbitals and transition energies for silicon (111) and (100) surfaces covered with a monolayer of oxygen (in eV).

Orbital energies	Transition energies	Final states
UPS	ELS	
-8.3	3.5	-4.8
?	5.0	?
-11.9	7.2	-4.7
-15.1	11	-4.1
-18.4	?	
(-28)	23	(-4.6)

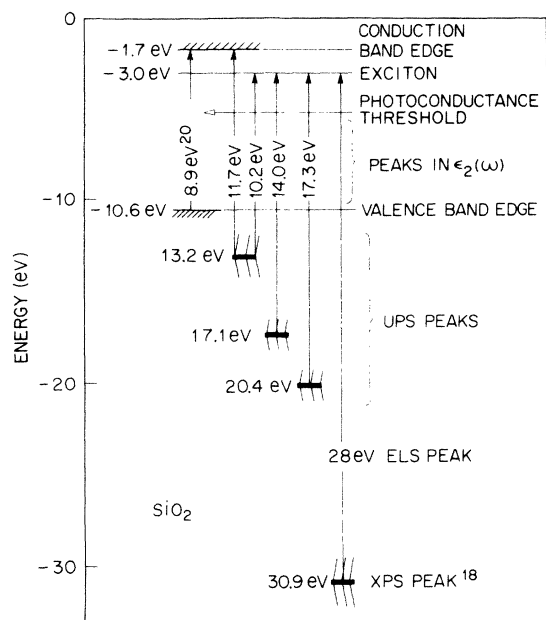


FIG. 8. Experimentally observed electron energy levels and transitions for amorphous SiO₂. The results of five different experimental methods lead to a consistent picture of the electronic-term scheme in SiO₂.

tions of SiO₂ can be identified and therefore the energies of the final states can be determined. In Fig. 8 we demonstrate that the results of five different experimental methods (XPS,²⁰ UPS, ELS, optical reflectivity,¹⁵ and photoconductivity)²¹ lead to a consistent picture of the electronic orbitals and the observed transitions of SiO₂. For a greater accuracy the transition energies in Fig. 8 were taken from the peaks in the dielectric function, $\epsilon_2(\omega)$. This function was calculated by H. R. Philipp from his measurement of the optical reflectivity of SiO₂ between 2 and 25 eV. Very little arbitrariness is involved in the association between UPS peaks and the observed transitions, since the final state should be between the Fermi level and the vacuum level.

It has already been pointed out by Reilly²² that the final state for the 10.2-eV transition (10.7 eV in the loss spectrum) may be an exciton with an electron orbital resembling the oxygen 3s orbital. The reader is referred to this paper²² for a detailed discussion and further references. Our data strongly suggest that this exciton is also the final state for the other transitions observed in ELS and optical reflectivity (Fig. 8). It is especially satisfying that the 28-eV transition from the oxygen 2s state also fits in this picture. This proves that transitions from oxygen-*s* electrons are seen in ELS and provides additional confirmation of our interpretation of the energy-loss data for both

SiO₂ and for adsorbed oxygen. According to the photoconductivity measurements of DiStefano and Eastman²¹ the band gap of SiO₂ is 8.9 ± 0.2 -eV wide. The valence band edge relative to the vacuum level was determined from the photoemission threshold to be -10.2 eV.²¹ Our data (see Fig. 3) suggest a slightly lower value of -10.6 eV and the conduction band edge is therefore calculated to be at -1.7 eV. The final state for the 11.7-eV transition could therefore be assigned to the conduction band edge (see Fig. 8) as proposed earlier by Reilly.²² The possibility of the final state being a higher exciton state near the conduction band edge should however not be excluded since the line shape is a broadened peak and not the continuum threshold expected for the conduction band edge which would appear approximately as a broadened-step function.

As in the case of adsorbed oxygen, the peaks in the UPS spectrum can be qualitatively interpreted in terms of molecular orbitals. A similar attempt has already been made by DiStefano and Eastman.¹⁵ The positions of our photoemission peaks are in general agreement with their results. However, we were not able to reproduce the high-energy shoulder on the -13.2-eV peak which played an important role in their interpretation. In none of our spectra obtained after various oxidation processes with background gas effects minimized was this shoulder observed.

DiStefano and Eastman interpreted their photoemission spectrum by comparing it with an artificially stretched Si-O-Si molecule and to the results of a crude linear combination of atomic orbitals-molecular orbitals (LCAO-MO) calculation of the SiO₂ valence-band structure.²² Both comparisons suggest that the energies of the two "nonbonding" orbitals are close together. The calculated orbital energies in the LCAO-MO model of Reilly,²² however, differ from the experimental values by 3-7 eV. Their prediction that the energies of the "nonbonding" (*a*₁ and *b*₁) orbitals are separated by ~2 eV can therefore not be taken too seriously. In the stretched Si-O-Si molecule which corresponds to the environment of oxygen in the β -cristobalite structure, the two nonbonding *p*-orbitals of oxygen are degenerate due to the *D*_{3d} symmetry of the nearest-neighbor environment of the oxygen. However, in amorphous SiO₂ the Si-O-Si bond angle is ~144° and the symmetry is therefore *C*_{2v}. Rather than considering the stretched Si-O-Si linear configuration, we prefer to compare our results to a molecule of the same symmetry such as H₂O. This comparison has already been applied by Hagstrum and Becker in order to explain the surface orbital energies of chalcogenides²³ adsorbed on nickel. It should be even more justified in the case of silicon where no *d* electrons complicate the picture. The Si-H and

TABLE II. Electron energies and transition energies of SiO₂ (in eV). The less accurate transition energies determined from the peak positions in the loss spectra are given in brackets. The final state at -3 eV is assumed to be an exciton while the suggested final state at -1.5 eV might be either a higher exciton or the conduction bond edge.

Orbital energies (UPS, XPS)	Transition energies $\epsilon_2(\omega)$ (ELS)	Final states	Orbital energies	Bond character of H ₂ O
-13.2	{ 10.2 (10.7) 11.7 (12.5)	-3.0 -1.5	-12.6	1b ₁ (2p π)
-17.1	14.0 (14.5)	-3.1	-14.4	3a ₁ (2p π^b)
-20.4	17.3 (17.8)	-3.1	-18.4	1b ₂ (2p σ)
...	21 Plasmon	...		
...	25			
-30.9 ¹⁵	28	-2.9	-32.2	2a ₁ (2s)

Si-O bond energies differ only by 6% and the difference in the electronegativity of hydrogen and silicon is small. The orbital energies of H₂O²⁴ and orbital symmetries are given in Table II. The energies agree surprisingly well with the energies found for SiO₂. As molecular-orbital calculations²⁴ show, the 1b₁ orbital is perpendicular to the H-O-H plane and consists entirely of the oxygen 2p_y orbital with no contribution from either p_x, p_z, or s orbitals. The 1b₁ orbital is therefore nonbonding and a close agreement of the energies in H₂O and SiO₂ is expected. We therefore consider the -13.2-eV peak in SiO₂ as being due to excitation from this nonbonding orbital. The 3a₁ orbital of H₂O is sometimes referred to as being nonbonding as well since it is not directed along the O-H bond. It contains contributions from hydrogen 1s and oxygen 2s and 2p_x electrons.²⁴ The charge density is concentrated between the two hydrogen atoms. This orbital 3a₁ is therefore responsible for the H-H bond. The 1b₂ orbital is constructed from hydrogen 1s and oxygen 2p_x electrons. Both the energies of the 3a₁ and the 1b₂ orbitals should therefore be sensitive to the bond angle and larger deviations of the SiO₂ values from the H₂O values are expected in agreement with the experimental results. We therefore believe the assignment in Table II to be correct.

V. CONCLUSIONS

There is now a large amount of data for oxygen adsorbed on silicon obtained from Auger, surface-vibration, photoemission, and energy-loss spectroscopies. These data show that the vibrational modes and the electronic properties of adsorbed oxygen are very different from oxygen in bulk SiO₂. The oxide formation occurs under well established conditions, such as heat treatment of an oxygen-covered surface,⁷ exposure to high pressures, simultaneous exposure and electron bombardment, or bombardment with oxygen ions. The latter method has been found to be convenient to form an SiO₂ layer involving much less than a

monolayer of silicon surface atoms. The photoemission-difference spectrum even for these small oxygen concentrations is (apart from a minor shift in the orbital energies) that of bulk SiO₂ (Fig. 4). The observed differences in the spectra for adsorbed oxygen and SiO₂ are therefore not caused by different concentration of the oxygen atoms. Furthermore, the spectra of oxygen in the bulk-oxide state, i. e., in a single-atom bridge position between two nearest-neighbor silicon atoms, seem to be not very sensitive to the considerable strain that must be involved in these bonds when only part of the silicon atoms are oxidized. We consider it highly unlikely that any model for the adsorbed oxygen involving bonds of an oxygen atom to nearest-neighbor silicon atoms could explain the observed spectra. Such a model has been recently proposed by Meyer and Vrakking.²⁵ They assume that oxygen dissociates during adsorption, one of the atoms breaks the silicon-silicon bond between a silicon surface atom and the nearest neighbor in the second layer, while the other connects the dangling bond of the surface atom with the next surface atom. The strain involved in these bonds would then tend to shift the two surface atoms involved closer together. Thus, essentially two strained SiO₂-type bonds would result in their mechanism after adsorption of an O₂ molecule. As explained above our results do not favor this interpretation. It should further be mentioned that Meyer and Vrakking developed their model in order to explain their ellipsometric data and the apparent high polarizability of adsorbed oxygen. Recent experiments on cleaved surfaces, however, showed that Meyer and Vrakking may have actually observed the simultaneous occurrence of adsorbed oxygen and SiO₂ which occurs on cleaved surfaces with low-step densities in the presence of oxygen ions (e. g., produced by an ion gauge).

The majority of all experimental results especially the number and frequency of the surface vibrations and the four p-like electron orbitals of the adsorbed oxygen are in agreement with a model

of a peroxide bridge connecting nearest-neighbor surface atoms originally proposed by Green and Maxwell,²⁶ On the other hand no experimental results have been found that could only be interpreted by assuming the peroxide bridge. Therefore, at present we consider the peroxide-bridge model for adsorbed oxygen as the most likely of the models that have been discussed so far.

ACKNOWLEDGMENTS

It is a pleasure to acknowledge a number of helpful discussions with J. A. Appelbaum, G. E. Becker, H. D. Hagstrum, and J. C. Phillips. The technical assistance of S. B. Christman and of E. E. Chaban is also greatly appreciated.

*Present address: Kernforschungsanlage, Jülich, Germany.

¹H. Ibach and J. E. Rowe, *Phys. Rev. B* **9**, 1951 (1974).

²H. Ibach, K. Horn, R. Dorn, and H. Lüth, *Surf. Sci.* **38**, 433 (1973). References to the earlier work are given in this paper.

³R. Dorn, H. Lüth, and H. Ibach (unpublished).

⁴J. E. Rowe (unpublished).

⁵J. E. Rowe, S. B. Christman, and E. E. Chaban, *Rev. Sci. Instrum.* **44**, 1675 (1973).

⁶H. Ibach and J. E. Rowe (unpublished).

⁷J. E. Rowe and H. Ibach, *Phys. Rev. Lett.* **32**, 421 (1974).

⁸A. M. Boonstra, *Philips Res. Rep. Suppl.* **3**, 1 (1968).

⁹J. J. Lander and J. Morrison, *J. Appl. Phys.* **33**, 2089 (1962).

¹⁰B. A. Joyce and J. H. Neave, *Surf. Sci.* **27**, 499 (1971).

¹¹J. E. Rowe and H. Ibach, *Phys. Rev. Lett.* **31**, 102 (1973).

¹²L. F. Wagner and W. E. Spicer, *Phys. Rev. Lett.* **28**, 1381 (1972).

¹³D. E. Eastman and W. D. Grobman, *Phys. Rev. Lett.*

28, 1378 (1972).

¹⁴J. A. Appelbaum and D. R. Hamann, *Phys. Rev. Lett.* **31**, 106 (1973).

¹⁵H. R. Philipp, *J. Phys. Chem. Solids* **32**, 1935 (1971).

¹⁶K. Siegbahn *et al.*, *ESCA applied to free molecules* (North-Holland, Amsterdam-London, 1969).

¹⁷J. D. Joannopoulos and M. L. Cohen, *Phys. Rev. B* **7**, 2644 (1973).

¹⁸F. C. Brown and O. P. Rustgi, *Phys. Rev. Lett.* **28**, 497 (1972).

¹⁹E. G. McRae, *Surf. Sci.* (to be published).

²⁰T. H. DiStefano and D. E. Eastman, *Phys. Rev. Lett.* **27**, 1560 (1971).

²¹T. H. DiStefano and D. E. Eastman, *Solid State Commun.* **9**, 2259 (1971).

²²M. H. Reilly, *J. Phys. Chem. Solids* **31**, 1041 (1970).

²³H. D. Hagstrum and G. E. Becker, *J. Chem. Phys.* **54**, 1015 (1971).

²⁴S. Aung, R. M. Pitzer, and S. I. Chan, *J. Chem. Phys.* **49**, 2071 (1968).

²⁵F. Meyer and J. J. Vrakking, *Surf. Sci.* **38**, 275 (1973).

²⁶M. Green and K. H. Maxwell, *J. Phys. Chem. Solids* **13**, 145 (1960).